www.icgst.com

# Amplitude Limitation Mechanisms in Quartz Crystal Oscillators : A Simulation Study Using Nonlinear Dipolar Method

F. CHIROUF[1], R. BRENDEL [2], M. ADDOUCHE [2], D. GILLET[2]
1 *Institut Universitaire de Technologie de Caen, Université de Caen Basse-Normandie*
Rue des Noës Davy, 14500 Vire, France
2 *Institut FEMTO–ST, UMR6174-CNRS.*
32, Avenue de l'Observatoire, 25044 Besançon Cedex, France.
farid.chirouf@unicaen.fr or farid.chirouf@free.fr
http://www.unicaen.fr/iutcaen.fr

## Abstract
This work presents some results in connection with the amplitude limitation mechanisms in quartz crystal oscillators circuits. These mechanisms were studied using the so called nonlinear dipolar method. This technique makes it possible to determine the close-loop operating conditions of the oscillator using open loop transient analyses. The well understanding of these limitation mechanisms should allow us to custom made quartz crystal oscillators, specifically for metrology and space applications.

***Keywords:*** *Dipolar method, dipolar impedance, quartz crystal oscillator, high-Q factor, time-domain analysis, SPICE.*

## 1. Introduction
The growing requirements of the scientific and technical applications, need increasingly powerful oscillators in terms of stability, precision and accuracy. These three criteria remain most determining in an oscillator whatever the application for which it is intended. The characteristics of quartz crystal oscillator such as the oscillation amplitude and frequency are strongly sensitive to the environment. Some of these influent factors are: the drive level of the resonator (isochronisme defect) [1], the electrode stress [2], the temperature effect [3], the acceleration sensitivity [4], the electroelastic effects and impurity relaxation [5], the ionizing radiations effects [6] , [7] the influence of a magnetic field [8].

This work focused on the study of amplifier amplitude limitation mechanisms of quartz crystal oscillators. We tent to achieve a non exhaustive classification of these different limitation mechanisms. In fact, the amplitude and to a lesser extent the frequency are determined through the non-linear behavior of the amplifier. From this point of view, we can classify the amplifiers from their amplitude limitation mechanisms such as saturation or cut off, soft or hard limitations, symmetrical or non- symmetrical limitation. The whole of these mechanisms were studied using the so called non-linear dipolar method [9]. This technique makes it possible to determine the close-loop operating conditions of the oscillator using open-loop analyses obtained with SPICE-like simulator [10], [11]. The well understanding of these limitation mechanisms should allows us to custom made quartz crystal oscillators, specifically for metrology and space applications. This paper is split on five sections. After an introduction on section one, the principales characteristics and performances of the quartz crystal oscillator are presented in section tow. Basic configuration and oscillation conditions of the quartz crystal oscillator are also illustrated in this section. Next section looks over the use of nonlinear dipolar method to analyze quartz crystal oscillator. Amplifier amplitude limitation mechanisms in quartz crystal oscillator are described in the forth section. Simulation results and discusions are also presented in this section. Finally, last section concludes this work and outlines the results of this study.

## 2. Quartz crystal oscillators circuits
### 2.1 Basic configurations and oscillation conditions
As shown in Figure.1 the oscillator may be split into two main elements:

- Element ***R*** represents the resonant circuit (quartz crystal). Its main task is to fix the greatest part of the oscillation frequency.
- Element ***A*** is the amplifier. It is composed of one or several non-linear components (transistors, diodes...). Its main task is to guarantee energy transfer and losses compensation on the one hand and to fix a limit to the amplitude oscillations on the other hand.

The oscillator operation is determined from the equality condition of $V_3$ and $V_1$ voltages (Figure 1). This condition is known as the *Barkhausen* criterion of oscillation [12]. What results in the equation system (1) implying the gain ($A$ and $R$) and also the phase ( $\phi_A$ and $\phi_R$ ):

$$\begin{cases} |A| \times |R| = 1 \\ \phi_A + \phi_R = 0 + 2k\pi : \quad k \in Z \end{cases} \tag{1}$$

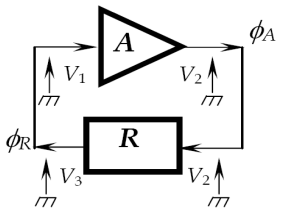


**Figure 1.** General representation of oscillator.

The *Barkhausen* criterion imposes an unitary gain and a null phase into the loop. Thus, we can differentiate three cases resumed in the Table 1. In a real oscillator, the amplifier non-linearities involve the gain reduction when the amplitude increases. This phenomenon brings back the loop gain towards the unit.

Table1. *Barkhausen* criterion and behaivoural oscillations.

| CONDITION | BEHAVIOURAL OSCILLATIONS |
|---|---|
| $\|A\|\|R\| < 1$ | oscillations diminish and the oscillator stops. |
| $\|A\|\|R\| > 1$ | oscillations are amplified and grow indefinitely. |
| $\|A\|\|R\| = 1$ | Steady-state is reached |

### 2.3 Electric model of the resonator

The equivalent electrical schematic of a quartz crystal resonator in the vicinity of its frequency of resonance is shown in Figure 2. This schematic suggested by VAN DYKE in 1925 [13] is drawn up from the fundamental equations that describe the resonator response subjected to a periodic excitation. This excitation which is applied on the resonator electrodes brings the vibrations of the quartz crystalline structure by inverse piezoelectric. The direct piezoelectric effect generates an electrical field between the resonator electrodes. Consequently, the resonator impedance change according to the frequency excitation.

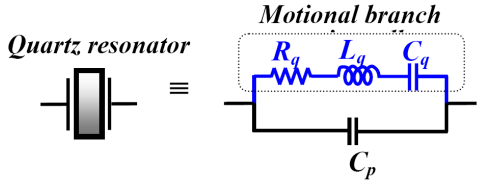


**Figure 2.** Electrical model of quartz crystal resonator.

W.G. CADY [14] demonstrates that the quartz crystal resonator spectrum is similar to the second order resonant circuit (Figure 2). The equivalent electrical schematic is composed of two parallel impedances. The first one consists on a motional branch which made up serial *RLC* circuit ($R_q$, $C_q$ and $L_q$). The second impedance corresponds to the capacitance ($C_p$) of the electrodes. The values of the motional branch elements depend on the crystal cut and the vibration mode of the resonator. While the oscillation angular frequency $\omega$ is very close to the resonant angular frequency $\omega_s$ of the resonator, we can write:

$$|\Delta\omega| = \omega - \omega_s \quad \text{with} \quad |\Delta\omega| << \omega_s \tag{2}$$

The total admittance $Y_q$ of the quartz is given by:

$$Y_q = \frac{1}{R_q + jX_q} = \frac{1}{R_q\left(1 + 2jQ_0\frac{\Delta\omega}{\omega_s}\right)} + jC_p\omega_s \tag{3}$$

The total reactance $X_q$ of the resonator worth zero for two frequencies, the *resonant frequency* $\omega_r$ and the *antiresonant frequency* $\omega_{an}$ :

$$\omega_r = \omega_s\sqrt{1 + \frac{R_q{}^2 C_p}{L_q}} \tag{4}$$

and

$$\omega_{an} = \omega_s\sqrt{1 + \frac{C_q}{C_p} - \frac{R_q{}^2\left(C_p + C_q\right)}{L_q}} \tag{5}$$

## 3. Non-linear Dipolar method

### 3.1 Quartz crystal oscillator representation from dipolar point of view

The non-linear dipolar method consists in representing quartz crystal oscillator by the motional branch of the resonator connected across a non-linear dipole amplifier (Figure 3). The oscillator behavior modeling is performed by analyzing separately the motional branch of the resonator and the amplifier part. Let's note that the parallel capacitance of the resonator is included on the amplifier part (Figure. 3). This disjoined analysis overcomes the expensive computing time imposed by the high-Q factor of the quartz resonator.

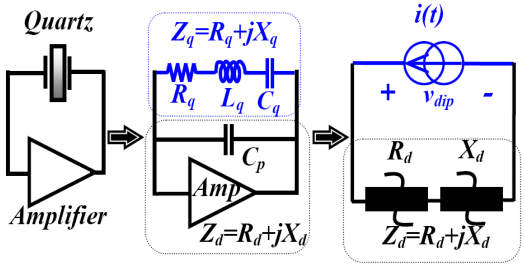


**Figure 3.** Dipolar representation of oscillator circuit.

The non-linear behavior of the amplifier can be determined in open loop by using transient analysis carried out by using an electrical simulation programme like SPICE. The nonlinear equivalent impedance of the amplifier is obtained by computing the complex impedance of the non-linear dipole ($R_d + jX_d$). The simulator results allow us to determine accurately the nonlinear equivalent impedance of the amplifier, i.e. its impedance vs the frequency and amplitude. The analysis consists in seeking the closed loop solution by using a series of open loop dipolar analyses with an iterative algorithm. This method leads to an accurate calculation of the operating conditions of the oscillator [9]: frequency, amplitude, drive level in transient and steady-state operation, and also amplitude and phase noise spectra.

### 3.2 Dipolar analysis principle

The resonator is considered as an *RLC* serial circuit connected in parallel with the capacitance $C_p$ which is included in the amplifier circuit. The impedance of the non-linear dipole amplifier strongly depends on the current amplitude and weakly depends on the current frequency. It can be represented by a nonlinear resistance $R_d$ in series with a nonlinear reactance $X_d$ (Figure 3). Because of the resonator high quality factor, the loop current is almost perfectly sinusoidal. Thus, it is possible to replace the *RLC* motional branch of the resonator by a harmonic current source $i(t)$ with amplitude a [9] and perform a set of transient analysis with increasing amplitudes by using an electrical simulation programme like SPICE (Figure 4 and 5). When the amplifier dipole is connected to the resonator, in steady-state operation, the nonlinear dipolar impedance $Z_d$ is exactly equal and opposite to the resonator impedance $Z_q$ [15]. The nonlinear differential equation of the oscillation loop current $i$ is given by (6) assuming that the condition $L_q >> L_d$ is always satisfied [9],.

$$\frac{d^2i}{dt^2}+\frac{1}{L_q}\left(R_q+R_d(a)\right)\frac{di}{dt}+\omega_q{}^2\left(1-\frac{L_d(a)}{L_q}\right)i=0 \quad (6)$$

Where $\omega_q$ is the series resonance angular frequency and $a$ is the amplitude of the harmonic current source. The solution of equation (6) takes the form (7) where $a(t)$ and $\phi(t)$ are slowly varying functions of time:

$$i(t)=a(t)\cos\left(\omega_0 t+\phi(t)\right) \quad (7)$$

By performing a Fourier analysis of the voltage across the dipole, it is possible to obtain the complex impedance $Z_d$ as a function of the current amplitude $a$. Equation (6) admits an increasing amplitude solution when the damping term is negative at low motional current amplitude. Then the start-up oscillation condition is given by:

$$R_d+R_{ds}<0 \quad (8)$$

Where $R_{ds}$ is the value of the dipolar resistance at very low current amplitude.

The dipolar resistance increases as the oscillation amplitude increases and the steady-state is obtained when:

$$R_q+R_0=0 \quad (9)$$

with $$R_0=R_d(a_0) \quad (10)$$

where $a_0$ is the steady-state oscillation amplitude. In this case, the oscillation angular frequency is given by (11) [9]:

$$\omega_0^2\approx\omega_q^2\left(1-\frac{L_d(a_0)}{Lq}\right) \quad (11)$$

The second order differential equation (9) can be transformed into a first order non-linear system, the solution of which gives the motional current amplitude and frequency transient as well as their steady-state operation values [9].

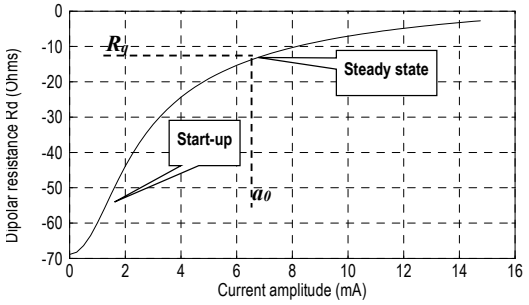


**Figure 4.** Amplifier nonlinear dipolar resiatance $R_d$ vs current amplitude $a$.

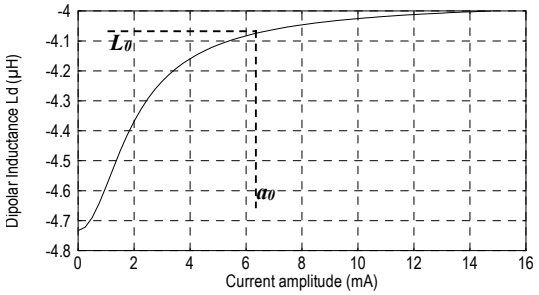


**Figure 5.** Amplifier nonlinear dipolar reactance $L_d$ vs current amplitude $a$.

## 4. Amplitude Limitation mechanisms in quartz crystal oscillators from dipolar analysis point of view

In oscillator circuits, the oscillation amplitude is basically determined by the non-linear behavior of the amplifier part. From this point of view, the amplifier circuits can be split in to several categories such as: bandwidth limitation, saturation or cut-off, soft or hard limitations, symmetrical or nonsymmetrical limitation, with possible combination of these various limitation mechanisms.

We can classify the amplifiers according to several criteria but it is essential to indicate some key properties of the amplifiers. As figure 6.a shows it, $Z_1$ and $Z_2$ are respectively the input and output

impedance of the amplifier. $Z_3$ represents the feedback impedance which include the parallel capacitance $C_p$. Although it is possible to include the $Z_3$ effect into the $Z_1$ and $Z_2$ impedances, it is more judicious to keep it out of these input and output impedances because of the particular part that $C_p$ play in the dipolar impedance. The amplifier can be represented either by a controlled voltage source or a controlled current source (Figure 6.b). Let us note that the voltage reference node is not necessary the circuit ground (Figure 6.a and 6.b). We can obtain the general expression of small-signal dipolar impedance by replacing the resonator motional branch with a current source having the same frequency (Figure 6.b). By expressing the dipolar voltage $v_{dip}$ according to the loop current $i$, we obtain the small-signal dipolar impedance as:

$$Z_{ds} = Z_1 + Z_2 - GZ_1Z_2 \qquad (12)$$

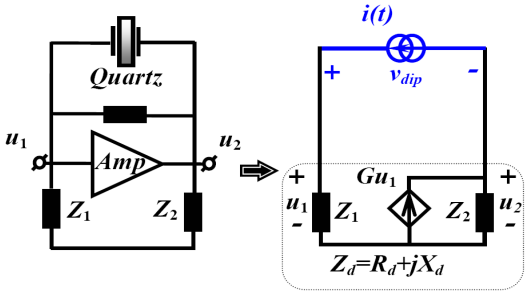


**Figure 6.** Amplifier representation in quatrz crystal oscillator : (a) General representation, (b) Dipolar reduction.

From the dipolar analysis point of view, the transconductance $G$ may have a real or complex value and may be linear or non-linear. In addition, the whole variables of the right hand side of equation (12) might be function of the current amplitude $a$. So that the nonlinear dipolar impedance takes the form:

$$Z_d(a) = R_d(a) + jX_d(a) \qquad (13)$$

### 4.1 Soft saturation limiting

The Van der Pol oscillator (Figure 7) is a simple example of soft limitation mechanism.

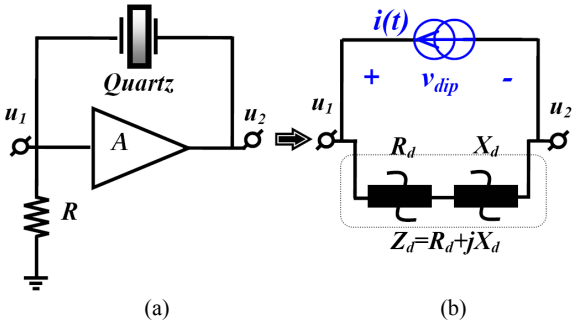


**Figure 7.** Van der Pol oscillator : (a) General representation, (b) Dipolar reduction.

In this case, we can demonstrate that the limitation is due to the nonlinear transfer function (14) of the amplifier as shown Figure 8.

$$u_2 = Au_1\left(1 - \varepsilon u_1 2\right) \qquad (14)$$

The small-signal gain $A$ and the non-linear coefficient $\varepsilon$ are supposed real and positive. We can demonstrate in this case that the nonlinear impedance (Figure.9) takes the form:

$$Z_d = (1 - A)R + \frac{3A\varepsilon R^3 a^2}{4} \qquad (15)$$

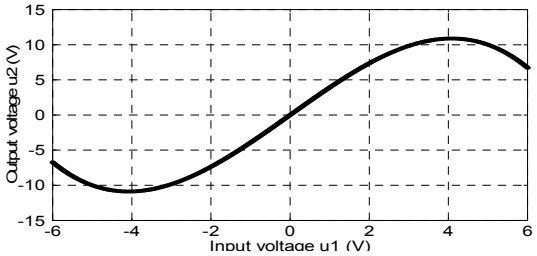


**Figure 8.** DC transfer function (Soft saturation case). (Values used : $A = 4$, $R = 100\ \Omega$, $\varepsilon = 0{,}02\ V^{-2}$)

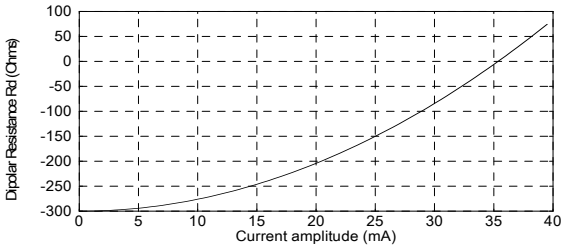


**Figure 9.** Dipolar resistance vs current amplitude $a$. (Soft saturation case)

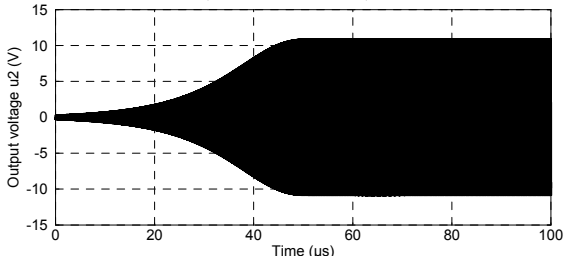


(a)

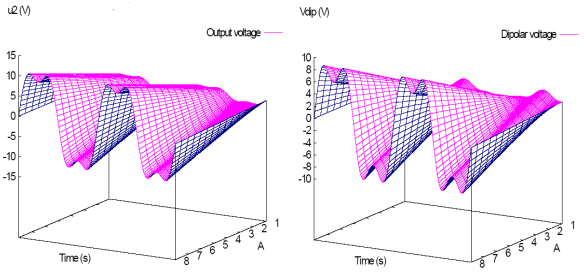


(b) (c)

**Figure 10.** Soft saturation case : (a). Transient Output voltage, (b) Output voltage waveform vs the gain $A$, (b) Dipolar voltage waveform vs the gain $A$.

As the amplitude increases, the impedance $Z_d$ remains real and increases according to a parabolic law (Figure 9). This is true as long as the amplifier does notcomprise a reactive element. The transient analysis of the output voltage it is shown in Figure 10.a. The sinusoidal signal that is injected into the input of the amplifier is deformed as it is shown in Figure 10.b and 10.d. Thus, the gain variation may also deforms the signal shape at the output $u_2$ and also across the resonator electrodes (dipolar voltage $v_{dip}$).

### 4.2 Hard saturation limiting

In this subsection, we consider the oscillator configuration of the Figure 6 with an amplification gain $A$ which is real, linear and symmetrically saturated (Figure 11). We also assume that the voltage amplifier is ideal and have null output impedance. The nonlinear transfer function of the amplifier is defined with the following conditions:

$$\begin{cases} -U_0 \le u_1 \le +U_0 \quad \Rightarrow \quad u_2 = Au_1 \\ u_1 \le -U_0 \quad \Rightarrow \quad u_2 = -U_{sat} \\ u_1 \ge +U_0 \quad \Rightarrow \quad u_2 = U_{sat} \end{cases} \tag{16}$$

This expression shown that the start-up dipolar impedance is a constant, real and negative as long as the gain $A$ is higher than the unity. As the loop current amplitude $a$ increases, the output voltage $u_2$ reaches the saturation level and becomes square wave (Figure 12.b) when the dipolar voltage is deformed (Figure 12.c). We compute the dipolar impedance according to the loop current amplitude $a$ by considering the fundamental harmonic.

At it is shown Figure 12.a, the dipolar impedance becomes nonlinear as long as the amplitude exceeds the limit $a_L$ which is expressed as:

$$a_L = \frac{V_{sat}}{A \times R} \tag{17}$$

As no reactive element is present in the circuit, the dipolar impedance remains purely real ( $X_d \approx 0$). In addition, the expression of the start-up dipolar impedance (12) demonstrates that it is impossible to use an inverter amplifier ($A < 0$) when the input and output impedances are real.

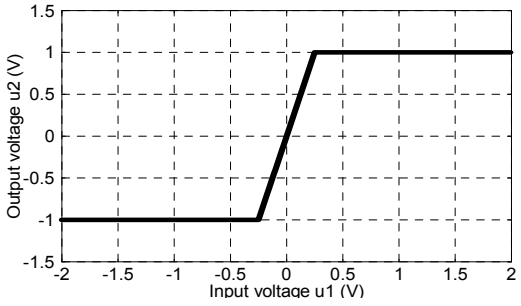


**Figure 11.** DC transfer function (Hard saturation case).

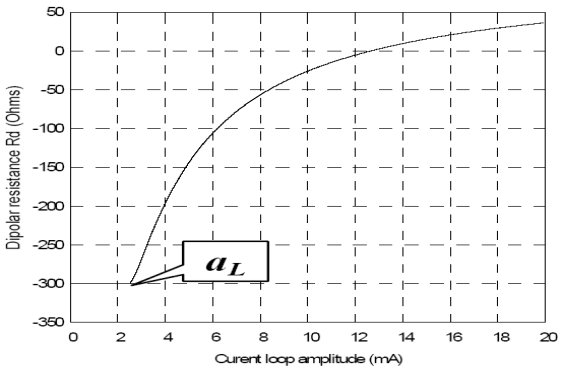


(a)

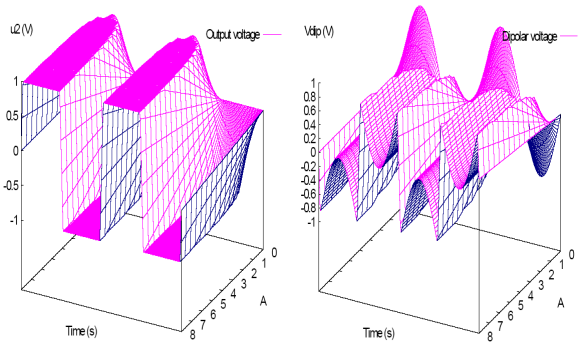


(b) (c)

**Figure 12.** Hard saturation case: (a) Dipolar resistance, (b) Output voltage waveform vs the gain $A$, (c) Dipolar voltage waveform vs the gain $A$.

### 4.3 Cutoff limitation

The cut-off limitation is often implied in the oscillators. The amplifier transfer function (Figure 13.a) is given in this case by the following equation system:

$$\begin{cases} u_1 \le -U_0 \quad \Rightarrow \quad u_2 = 0 \\ u_1 \ge -U_0 \quad \Rightarrow \quad u_2 = \left(u_1 + U_0\right) \end{cases} \tag{18}$$

With this kind of limitation, the dipolar voltages and also the voltages at the output are not any more symmetrical (Figure 13.c and 13.d). As in the case of thesaturation mechanism, the dipolar start-up impedance remains constant as long as the loop current amplitude stays below a threshold value. This value is indicative of reaching the cut-off voltage. Starting from this threshold voltage, dipolar impedance increases according to the growing of loop current amplitude (Figure 13.b). Thus, this value corresponds to the beginning of the amplifier non-linear behavior.

This study does not considering the bandwidth limitation mechanism. Because in the case of amplifier configuration (without reactive component suh as Van der Pol oscillator) the dipolar resistance is pratically unaffeted by bandwidth limitation mechanism of the amplifer as shown in Figure 14.

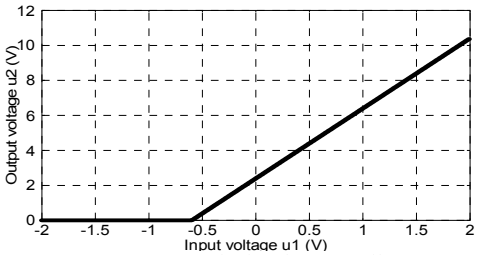


**Figure 14.** DC transfer function (Cut-off case).

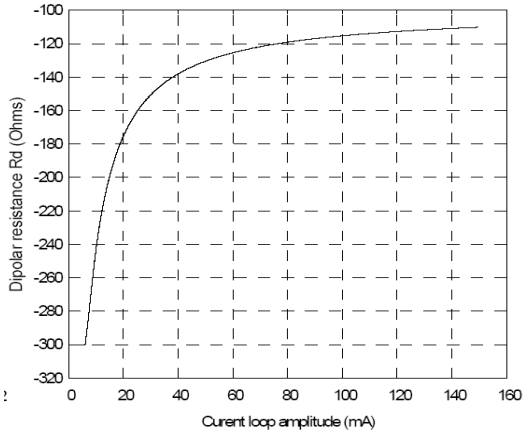


(b)

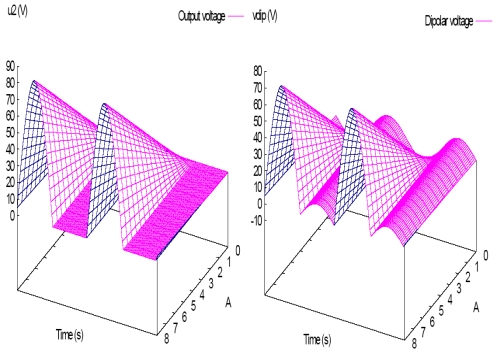


(c) (d)

**Figure 13.** Cut-off case: (a) Dipolar resistance, (c) Output voltage waveform vs the gain $A$, (d) Dipolar voltage waveform vs the gain $A$.

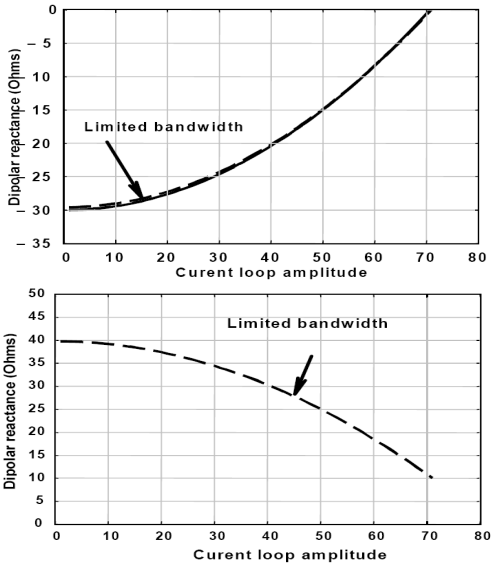


**Figure 14.** Dipolar impedance in the case of bandwidth limitation. (Van der Pol oscillator : oscillation frequency:10 MhZ, cutoff frequency : 100 Mhz)

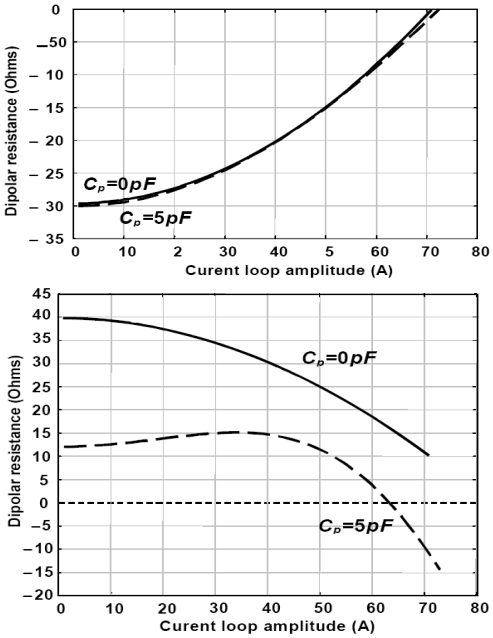


**Figure 15.** Parallel capacetance effect on the dipolar impedance.

As it was mentioned before, the parallel resonator capacitance $C_p$ is included into the amplifier part. However, it is not trivial to give a sense to the dipolar impedance of this capacitance separately since it is crossed by a non-sinusoidal current. Figure 15 gives us the parallel capacitance effect on the dipolar impedance of a limited bandwidth Van der Pol amplifier. We can observe that the parallel capacitance has a weak influence on the real part of the dipolar impedance but it completely changes the dipolar reactance.

### 4.4 Transconductance amplifier with cutoff limitation mechanism

Several simulations performed on transconductance amplifiers (Figure 16) with different limitation mechanisms have shown that the input and output impedances (or time constants) have similar effects on the nonlinear dipolar impedance. Thus, the attention will be focused only on the cut-off limiting mechanism often involved in the oscillator circuits. In this case, the nonlinear transconductance represented in Figure 16.a is defined by the conditions (19).

$$\begin{cases} u_1 \le -U_0 \quad \Rightarrow \quad i_G = 0 \\ u_1 \ge -U_0 \quad \Rightarrow \quad i_G = -G(u_1 + U_0) \end{cases} \tag{19}$$

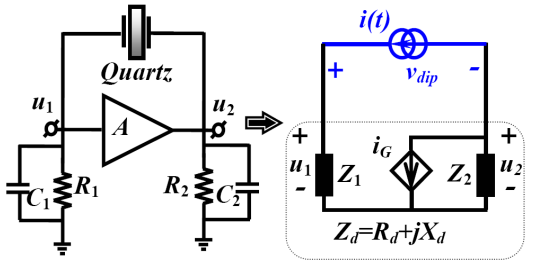


(a)

**Figure 16.** Transconductance amplifier :
(a) General representation, (b) Dipolar reduction.
($G$ =100 mA/V, $C_1$=$C_2$=75 pF, $R_1$= 100 Ω, $R_2$=1000 Ω)

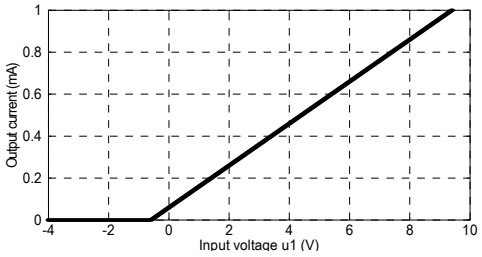


**Figure 17.** DC transfer function
(Transconductance with cutoff limiting).

The output and dipolar voltage waveforms of the transconductance amplifier with cut-off limiting for a given pair of impedances $Z_1$ and $Z_2$ are shown in Figure 18.

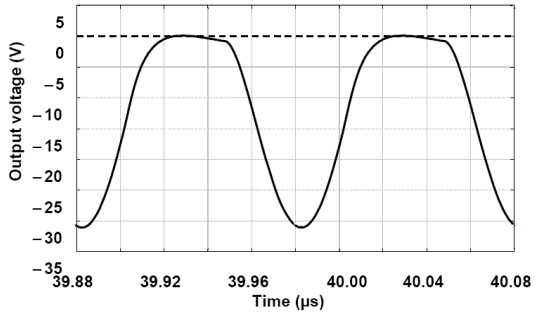


(a)

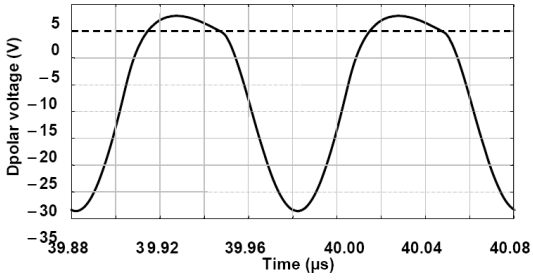


(b)

**Figure 18.** Transconductance amplifier waveforms (cutoff case): (a) Output voltage, (b) Dipolar voltage.

As it shown on Figures.19, for small signal current amplitude the dipolar resistance and reactance of the amplifier keep the same values. As the amplitude quite different location. The parallel capacitance strongly modifies both the dipolar resistance and reactance of the amplifier (Figure.19). The negative reactance corresponds to a positive frequency shift that can become very large if the resonator motional inductance $L_q$ is not much greater than the dipolar inductance $L_d$ of the amplifier. Let us note in addition that the input and output impedances of the amplifier stage may significatively modify the dipolar behavior of the oscillator in study.

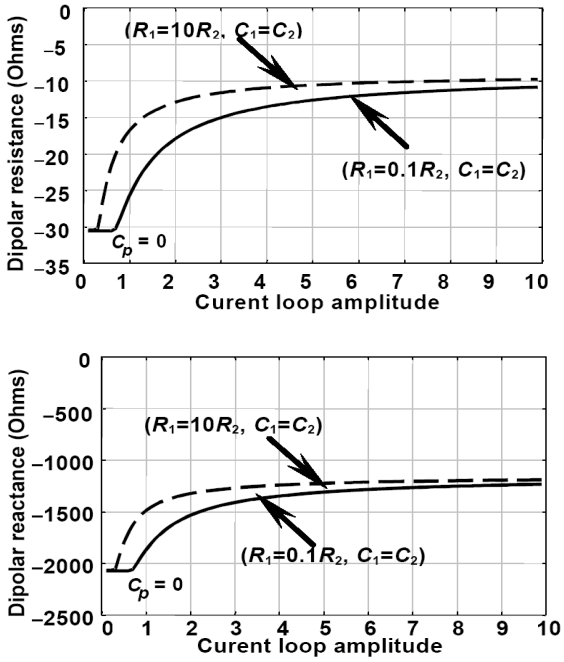


**Figure 19.** Dipolar impedance (cutoff case).

## 5. Conclusion

The nonlinear dipolar analysis allowed us to study the most important and influent amplifier parameters on the oscillator operation. This work demonstrates the efficiency of this nonlinear analysis method that is well adapted to the quartz crystal oscillators. All the simulations are achieved using dedicated software (ADOQ) whose efficiency and accuracy have been assessed experimentally [9].

## 5. References

[1] J. J. Gagnepain. Mécanismes non linéaires dans les résonateurs à quartz : Théories, expériences et applications métrologiques. PhD thesis, Université de Besançon, 1972.

[2] E. P. Ernisse. Quartz resonator freqency shifts arising from electrode stress. In proceedings of the 29th IEEE–AFCS. 1975.

[3] M. E. Frerking. *Crystal oscillator design and temperature compensation*. New York: Van Nostrand, 1978.
[4] J. M. Przyjemski. Improvement in system performance using a crystal oscillator compensated for acceleration sensitivity. In proceedings of the 32nd IEEE–AFCS, 1978.
[5] R. Brendel, J. J. Gagnepain. Electroelastic effects and impurity relaxation in quartz resonators. In proceedings of the 36th IEEE–AFCS. 1982.
[6] R. Chévralis. Effets des rayonnements ionisants sur les résonateurs à quartz. Rapport technique no 32/7132 PN; ONRA.1986.
[7] M. Brunet. Etude expérimentale sur la dérive des OUS spatiaux soumis aux irradiations. Rapport CNES, 1990.
[8] R. Brendel. Influence of a magnetic field on quartz crystal resonators. IEEE Trans. Ultrason., Ferroelect., Freq. Contr., vol. 43, pp. 818–831, 1996.
[9] M. Addouche, R. Brendel, D. Gillet, N.Ratier, F. Lardet-Vieudrin, and J. Delporte. Modelingof Quartz crystal oscillators by using nonlineardipolar method. IEEE Trans. UFFC, vol. 50, pp. 487-495, 2003.
[10] L. Nagel. SPICE2: A computer program to simulate semiconductor circuits. UCB/ERL M 520. Electron. Res. Lab.,Univ.California at Berkeley, USA. 1975.
[11] T. Quarles. The SPICE 3 implementation guide. UCB/ERL M 89/44. Electron. Res. Lab., Univ. California at Berkeley. USA. 1989.
[12] H. Barkhausen, Lehrbuch der Elektronen–Rohre, 3.Band, RÄuckkopplung, Verlag S. Hirzel,1935.
[13] Van Dyke. The electric network equivalent of piezoeletric resonator. Phys. Rev., vol. 25, pp. 895,1925.
[14] W. G. Cady. The piezoelectric resonator. Phys. Rev., vol. 17, pp. 531, 1921.
[15] K. Kurokawa. Some basic characteristics of broadband negative resistance oscillator circuits. Bell System Technical Journal. vol.48. 1937-1955. Bell Laboratories, Murray Hill, USA, July–August 1969.